

Fermion-induced quantum action of vortex systems

Kurt Langfeld^a, Laurent Moyaerts^a, Holger Gies^b

^a Institut für Theoretische Physik, Universität Tübingen
D-72076 Tübingen, Germany

^b CERN, Theory Division
CH-1211 Geneva 23, Switzerland

Abstract

The quantum action generated by fermions which are minimally coupled to abelian vortex background fields is studied in $D = 2+1$ and $D = 3+1$ Euclidean dimensions. We present a detailed analysis of single- and binary-vortex configurations using the recently developed method of worldline numerics. The dependence of the fermion-induced quantum action on the fermion mass and the magnetic fluxes carried by the vortices is studied, and the binary-vortex interaction is computed. Additionally, we discuss the chiral condensate generated from a dilute gas of vortices in the intermediate fermion mass range for the case $D = 3+1$. As a byproduct, our findings provide insight into the validity limits of the derivative expansion, which is the standard analytical approach to inhomogeneous backgrounds.

PACS: 12.20.-m, 11.15.Ha

keywords: worldline, fermion-induced effective action, vortex, Monte-Carlo simulation.

1 Introduction

The dynamics of surfaces plays an important role in many fields of physics ranging from solid state physics and chiral quantum field theories [1, 2, 3] to string theory [4]. The so-called vortices, $d - 2$ -dimensional surfaces of the d -dimensional space, are of particular interest in view of their phenomenological importance: in solid state physics, freely moving vortices give rise to a non-vanishing conductance of high T_c -superconductors, thereby limiting their technical applicability [5]. In the context of Yang-Mills theory, it has recently been observed in lattice gauge simulations that, in the continuum limit [6], the Yang-Mills vacuum is populated by center vortices the core of which can be detected in a certain gauge by a projection technique [7, 8]. A random gas of these vortices can grasp the essence of quark confinement at zero temperature, and the deconfinement phase transition at finite temperatures can be understood as a vortex de-percolation transition [9, 10]. Although rigorous estimates signal that the core size of the full (unprojected) field configurations is spread over the whole spacetime [11], an effective vortex model supplemented by a particular core size describes certain low-energy observables remarkably well [12, 13].

In many applications, the surfaces appear as classical background fields (solitons) of an underlying field theory. The surface properties as well as the surfaces' interactions are determined by thermal and quantum fluctuations, respectively [14, 15]. In the context of the layered superconductors, the spectrum of the quasi-particles encodes phenomenologically relevant information of the vortex background [16, 17]. In the context of Yang-Mills theory, a deep knowledge of the interplay of quarks with vortex-like solitons would help to describe hadron properties in the vortex picture.

The determination of the vortex free energy generically requires the calculation of functional determinants where the vortex profile enters as a background field. Whereas the eigenvalue problem of the single-vortex case with a θ -function profile can be solved analytically [18], a numerical treatment seems inevitable for realistic profiles and multi-vortex configurations. One possible technique aims at the numerical integration of a Klein-Gordon or Dirac type of equation associated with the differential operator under consideration. For example, in [14, 15], this approach has been further developed and the numerical burden has been reduced to a quantum mechanical computation of bound-state energies and scattering phase shifts; in particular, the usually delicate issue of renormalization can advantageously be inherited from standard perturbation theory in this approach. The disadvantage of this approach is that numerical complications increase with the degree of complexity of the background field; up to now, only highly symmetric backgrounds have been treated (see [19] and [20] for the single-vortex case). In this work, we put forward a recently proposed numerical technique [21, 22] which is based on the "string-inspired" worldline method [23]. In this formalism, the effective action (functional determinant) is represented in terms of first-quantized particle path-integrals, which have turned out to be highly convenient for analytical computations involving constant background fields (see [24] for a review). In our numerical realization of this formalism, Monte-Carlo techniques can be exploited to estimate expectation values of background-field dependent operators with respect to scalable worldline ensembles, so-called *loop clouds*. This worldline numerical scheme is formulated

in coordinate space, which facilitates a transparent renormalization, since the divergencies are associated with local operators in coordinate space and the required counterterms can easily be read off. The most important advantage of this formalism is marked by the fact that the numerical algorithm can be realized without any reference to the specific choice of the background field. In particular, a high degree of symmetry of the background is not required at all; on the other hand, if a symmetry is present, it can, of course, be exploited for reducing numerical efforts. Most recently, this technique was adapted for worldline loops on a cubic lattice, most convenient in the case of lattice gauge simulations [25]. Therein, it was pointed out that a random walk easily generates loop clouds with the appropriate measure required for the worldline approach.

In this paper, we will explore the free energy of vortex-type solitons, being supported by a $U(1)$ gauge field which is minimally coupled to a fermion. We will discuss the case of $2+1$ and $3+1$ spacetime dimensions and restrict ourselves to vortex configurations which are static with respect to one or two directions of spacetime, respectively. The free energy will be studied for the single and the binary-vortex configuration. In the latter case, we will obtain the fermion-induced vortex-vortex interaction.

The paper is organized as follows: in the next section, the worldline approach to the fermion determinant is introduced and the renormalization procedure is discussed in detail for the case $D = 3 + 1$. The vortex configurations under investigation are introduced in section 3. In section 4, our numerical result for the single-vortex configuration is presented and compared with the estimate obtained from existing analytical studies. The binary-vortex interaction is presented in section 5. Fermion condensation due to a dilute gas of vortices is addressed in section 6. Conclusions are left to the final section.

2 Fermion determinants in the worldline approach

2.1 Setup

In this paper, we shall investigate the case of one flavor of a 4-component Dirac fermion in $D = 2 + 1$ and $D = 3 + 1$ spacetime dimensions. The fermion field is minimally coupled to a $U(1)$ gauge field $A_\mu(x)$, which is considered as a background field. The fermion-induced effective action Γ_{ferm} , which is a free-energy functional, determines the probabilistic weight $\exp\{-\Gamma_{\text{ferm}}\}$. It is given by

$$\Gamma_{\text{ferm}} = - \ln \det(m - i\mathcal{D}), \quad \mathcal{D} := \not{\partial} + i\not{A}, \quad (1)$$

where m is the fermion mass, $\not{A} = A_\mu(x) \gamma_\mu$, and γ_μ are the anti-hermitean Euclidean γ -matrices, $\gamma_\mu^\dagger = -\gamma_\mu$. As a consequence, \mathcal{D} is hermitean.

Since the Dirac operator exhibits no spectral asymmetry in the 4-component formulation, the effective action is real, and we obtain in Schwinger proper-time regularization

$$\Gamma_{\text{ferm}} = \frac{1}{2} \int_{1/\Lambda^2}^{\infty} \frac{dT}{T} e^{-m^2 T} \text{Tr} \exp\{-\mathcal{D}^2 T\}, \quad (2)$$

where the scale Λ acts as a UV regulator. The idea of the worldline approach consists of rewriting Eq. (2) in terms of 1-dimensional path integrals (for a comprehensive review, see [24]). The worldline representation of Eq. (2) is given by

$$\Gamma_{\text{ferm}} = \frac{1}{2} \frac{1}{(4\pi)^{D/2}} \int d^D x_0 \int_{1/\Lambda^2}^{\infty} \frac{dT}{T^{(D/2)+1}} e^{-m^2 T} 4 \left\langle W_{\text{spin}}[A] - 1 \right\rangle_x, \quad (3)$$

where a gauge-field independent constant has been dropped, and we have defined the spinorial counter gauge factor of the Wilson loop including the Pauli term (spin-field coupling),

$$W_{\text{spin}}[A] = \frac{1}{4} \exp \left\{ i \int_0^T A_\mu(x) \dot{x}_\mu d\tau \right\} \text{tr} P_T \exp \left(\frac{1}{2} \int_0^T d\tau \sigma_{\mu\nu} F^{\mu\nu} \right). \quad (4)$$

Here $F^{\mu\nu}(x(\tau))$ is the field strength tensor, and $\sigma_{\mu\nu} := i[\gamma_\mu, \gamma_\nu]/2$ are hermitean Dirac algebra elements. The average $\langle \dots \rangle_x$ in (3) is performed over an ensemble of closed worldlines, or *loop clouds*. A single loop is characterized by its worldline $x_\mu(\tau)$, $\tau \in [0, T]$ in D dimensions. P_T denotes path ordering with respect to the proptime T . The loops are centered upon a common average position,

$$x_0^\mu := (1/T) \int_0^T d\tau x_\mu(\tau), \quad (\text{“center of mass”}).$$

The loop ensemble is generated according to the Gaussian weight:

$$\exp \left[-\frac{1}{4} \int_0^T d\tau \left(\dot{x}_1^2 + \dots + \dot{x}_D^2 \right) \right]. \quad (5)$$

In practice, one greatly reduces the numerical work by generating a loop gas of unit proptime $T = 1$ only, and by producing loop ensembles for a given proptime $T \neq 1$ by rescaling. This numerical method is discussed in some detail in [21, 22].

Finally, we point out that the symmetry of the background field can easily be exploited to reduce the numerical burden. In our case, the background field is static with respect to $D - d$ space-time dimensions, i.e., the gauge field depends only on the coordinates x_1, \dots, x_d , $d < D$. Since the weight of the loop clouds is Gaussian, the loop average in D dimensions can be evaluated by using $d < D$ dimensional loop clouds only, i.e.,

$$\left\langle F[A] \right\rangle_x = \frac{1}{\mathcal{N}} \int \mathcal{D}x_{1\dots d} F[A] e^{-\frac{1}{4} \int_0^T d\tau \left(\dot{x}_1^2 + \dots + \dot{x}_d^2 \right)}, \quad (6)$$

where

$$\mathcal{N} = \int \mathcal{D}x_{1\dots d} e^{-\frac{1}{4} \int_0^T d\tau \left(\dot{x}_1^2 + \dots + \dot{x}_d^2 \right)}.$$

In particular, it is sufficient for the examples discussed below to generate a single (large) 2-dimensional loop cloud to address the properties of static vortices in $D = 2 + 1$ and $D = 3 + 1$, respectively.

2.2 Renormalization

In the case of $D = 2 + 1$ dimensions, the proptime integration in Eq. (3) is finite at the lower bound. This implies that one might safely remove the regulator, i.e., $\Lambda \rightarrow \infty$, in this case. We therefore confine ourselves in this subsection to the case $D = 3 + 1$, where the fermion-induced effective action discussed above is actually the bare action and given by

$$\Gamma_{\text{ferm}}^{\text{B}} = \frac{1}{2} \frac{4}{(4\pi)^2} \int d^4x_0 \int_{1/\Lambda^2}^{\infty} \frac{dT}{T^3} e^{-m^2 T} \left\langle W_{\text{spin}}[A] - 1 \right\rangle_x. \quad (7)$$

For small values of the proptime T , the expectation value $\langle W_{\text{spin}}[A] - 1 \rangle_x$ can be calculated analytically for the case of a loop cloud with x_0 being the center of mass. One finds

$$\left\langle W_{\text{spin}}[A] \right\rangle_x = 1 + \frac{1}{6} F_{\mu\nu}(x_0) F_{\mu\nu}(x_0) T^2 + \dots, \quad (8)$$

where the ellipsis denotes higher-order invariants that can be formed out of the field strength tensor, its dual, and derivatives thereof. Rewriting (7) as

$$\Gamma_{\text{ferm}}^{\text{B}} = \frac{1}{8\pi^2} \int d^4x_0 \int_{1/\Lambda^2}^{\infty} \frac{dT}{T^3} e^{-m^2 T} \left\langle W_{\text{spin}}[A] - 1 - \frac{1}{6} F^2(x_0) T^2 \right\rangle_x \quad (9)$$

$$+ \frac{1}{6} \frac{1}{8\pi^2} \int_{1/\Lambda^2}^{\infty} \frac{dT}{T} e^{-m^2 T} \int d^4x_0 F^2(x_0), \quad (10)$$

we observe that the part (9) of $\Gamma_{\text{ferm}}^{\text{B}}$ is finite if the regulator is removed, $\Lambda \rightarrow \infty$. Using

$$\int_{1/\Lambda^2}^{\infty} \frac{dT}{T} e^{-m^2 T} = -\ln\left(\frac{m^2}{\Lambda^2}\right) - \gamma_{\text{E}} + \mathcal{O}\left(\frac{m^2}{\Lambda^2}\right), \quad (11)$$

(γ_{E} is the Euler constant), we neglect irrelevant terms which are suppressed by powers of $1/\Lambda^2$ in part (9) and (10) and obtain

$$\Gamma_{\text{ferm}}^{\text{B}} = \frac{1}{8\pi^2} \int d^4x_0 \int_0^{\infty} \frac{dT}{T^3} e^{-m^2 T} \left\langle W_{\text{spin}}[A] - 1 - \frac{1}{6} F^2(x_0) T^2 \right\rangle_x \quad (12)$$

$$- \frac{1}{48\pi^2} \left[\ln\left(\frac{m^2}{\Lambda^2}\right) + \gamma_{\text{E}} \right] \int d^4x_0 F^2(x_0). \quad (13)$$

The renormalized effective action Γ_{eff} is obtained by adding the bare ‘‘classical’’ action

$$\Gamma_{\text{eff}} = \Gamma_{\text{ferm}}^{\text{B}} + \frac{1}{4g_{\text{B}}^2} \int d^4x_0 F^2(x_0), \quad (14)$$

where g_{B}^2 is the bare coupling constant, and we enforce the renormalization condition

$$\frac{1}{g_{\text{B}}^2(\Lambda)} + \frac{1}{12\pi^2} \left[\ln\left(\frac{\Lambda^2}{\mu^2}\right) - \gamma_{\text{E}} \right] = \frac{1}{g_{\text{R}}^2(\mu)}. \quad (15)$$

Here $g_{\text{R}}(\mu)$ denotes the renormalized coupling at a given renormalization point μ , and we rediscover the QED β function $\beta(g_{\text{R}}^2) = \mu \partial_{\mu} g_{\text{R}}^2(\mu) = g_{\text{R}}^4/(6\pi^2)$. Inserting (12) and (15) into (14), the renormalized effective action is given by

$$\begin{aligned} \Gamma_{\text{eff}} &= \Gamma_{F^2} + \Gamma_{\text{ferm}}, \\ \Gamma_{\text{ferm}} &= \frac{1}{8\pi^2} \int d^4x_0 \int_0^{\infty} \frac{dT}{T^3} e^{-m^2 T} \left\langle W_{\text{spin}}[A] - 1 - \frac{1}{6} F^2(x_0) T^2 \right\rangle_x, \end{aligned} \quad (16)$$

$$\Gamma_{F^2} = \frac{1}{4} \left[\frac{1}{g_{\text{R}}^2(\mu)} - \frac{1}{12\pi^2} \ln \left(\frac{m^2}{\mu^2} \right) \right] \int d^4x_0 F^2(x_0). \quad (17)$$

In these equations, Γ_{F^2} denotes the renormalized Maxwell action; here we can impose fermion-mass-shell renormalization by choosing $\mu = m$, so that the log term in (17) drops out. In addition to the (trivial) classical term (17), worldline numerics provides us with an explicit answer for the renormalized fermion-induced quantum contribution $\Gamma_{\text{ferm}} = \int d^Dx \mathcal{L}_{\text{ferm}}$ given by (16).

The renormalization scheme employed here can easily be related to standard renormalization prescriptions for Feynman amplitudes. The latter are formulated, for instance, by considering the renormalized photon propagator $D_{\mu\nu}(p) = P_{\mu\nu} D(p^2)$ in the Landau gauge, where $P_{\mu\nu}$ is the transverse projector, and specifying a number R ,

$$R := \frac{\partial}{\partial p^2} D^{-1}(p^2) \Big|_{p^2=0}, \quad (18)$$

which determines the wave function renormalization constant in a particular renormalization scheme. Since the effective action Γ_{eff} given above represents nothing but the generating functional for one-particle irreducible Green's functions, it is related to the renormalized photon propagator by

$$\left(D^{-1} \right)_{\mu\nu}(x, y) = \frac{\delta^2 \Gamma_{\text{eff}}[A]}{\delta A_{\mu}(x) \delta A_{\nu}(y)}. \quad (19)$$

We observe that the part (16) does not contribute to the right-hand side of Eq. (18) in the limit $p^2 \rightarrow 0$; this leads us to the desired result

$$R = \frac{\partial}{\partial p^2} D^{-1}(p^2) \Big|_{p^2=0} = \frac{1}{g_{\text{R}}^2(\mu)} - \frac{1}{12\pi^2} \ln \left(\frac{m^2}{\mu^2} \right), \quad (20)$$

which determines the value of the coupling at any renormalization scale μ for a given value of R .

3 Vortex interfaces

The core of a vortex corresponds to a $D-2$ dimensional surface of D -dimensional Euclidean spacetime. The vortex field which we will discuss below is represented by a $U(1)$ gauge

potential $A_\mu(x)$. In an idealized case, the gauge potential is singular at the vortex surface and can locally be represented by a pure gauge. Considering a closed line \mathcal{C} , the vortex can be characterized by the holonomy

$$\exp\left\{i \oint_{\mathcal{C}} A_\mu(x) dx_\mu\right\} = \exp\{i \phi L\}, \quad (21)$$

where ϕ is the magnetic flux carried by the surface, and L is the linking number of \mathcal{C} with the $D - 2$ dimensional vortex surface. In the case $\phi = \pi$, the gauge potential describes a so-called center vortex in analogy to SU(2) Yang-Mills theory.

In many physical applications (for instance, in the context of center vortices in Yang-Mills theories) one observes that the vortex surface possesses a finite thickness d with respect to the directions perpendicular to the flux, implying that the gauge potential singularity in the surface is smeared. We point out that the physics of the extended object can be quite different from the physics of the idealized vortex. In the latter case, one removes the $D - 2$ dimensional vortex surface from the base manifold. Quantum fields are acting in the reduced coordinate space and obey certain constraints at the singular subspace. For purposes of illustration consider the case $\phi = 2\pi$. One expects that the free energy of the vortex is degenerated with the vacuum because the quantum fields of both cases are related by a gauge transformation (see [26] for an illustration at the 1-loop level). By contrast, in the case of the smeared vortex surface, the quantum fields experience the magnetic flux of $\phi = 2\pi$. Therefore one does not expect a degeneracy of the smeared vortex configuration with the vacuum.

In this first investigation, we will concentrate on plane vortex surfaces. For definiteness, we consider the gauge potential of a vortex with flux $\phi = \varphi\pi$ and core size d of the form

$$A_\mu(x) = \frac{\varphi}{2} \frac{1}{d^2 + x_1^2 + x_2^2} (x_2, -x_1, 0, \dots, 0)_\mu^T, \quad \mu = 1 \dots D. \quad (22)$$

Since the worldline approach is manifestly gauge invariant, any other choice of a gauge-equivalent configuration would give the same fermionic interface energy. The corresponding field strength is given by

$$F_{12}(x) = \frac{\varphi d^2}{[d^2 + x_1^2 + x_2^2]^2}. \quad (23)$$

In the case of $D = 2+1$ dimensions, the fermion-induced effective action is proportional to the extent L_t of the space-time in time direction,

$$\Gamma_{\text{ferm}}^{(3)} = E L_t = L_t 2\pi \int_0^\infty d\rho \rho \mathcal{L}_{\text{ferm}}^{(3)}(\rho), \quad (24)$$

where ρ is the radial coordinate of the xy -plane. E can be interpreted as the energy of the static vortex soliton. $\mathcal{L}_{\text{ferm}}^{(3)}(\rho)$ is a radial energy density, i.e., the amount of energy which is stored in a cylindric shell $[\rho, \rho + d\rho]$. In the case of $D = 3 + 1$ dimensions and at a given

time slice, the vortex core is given by a straight line of length L_z . The effective action is proportional to the extent $L_t L_z$,

$$\Gamma_{\text{ferm}}^{(4)} = \chi L_t L_z = L_t L_z 2\pi \int_0^\infty d\rho \rho \mathcal{L}_{\text{ferm}}^{(4)}(\rho), \quad (25)$$

where χ is the string tension of the vortex line in the 3D hypercube.

4 Quantum energy of the single-vortex configuration

4.1 The derivative expansion

The standard analytical approach to effective actions and quantum energies for nonhomogeneous backgrounds is the derivative expansion. Here, the desired answer is expanded in terms of a small parameter constructed from derivatives of the background field. In the present case, there are two options for the expansion parameter, which can symbolically be written as $\partial^2/m^2 \ll 1$ or $\partial^2/B(x) \ll 1$, i.e., the derivatives of the background field should be smaller than the fermion mass or the local field strength. It is remarkable that closed-form expressions at the next-to-leading order (NLO) level in $D = 2 + 1$ and $D = 3 + 1$ have been found in recent years which are applicable in both cases; only one of the conditions mentioned above has to be satisfied. The leading-order derivative expansion, which agrees with the Euler-Heisenberg effective Lagrangian for constant background fields, is given by [27, 28]

$$\mathcal{L}_{\text{ferm}}^{d0}(x) = C_{d0} \int_0^\infty \frac{dT}{T^\nu} e^{-m^2 T} [B(x)T \coth(B(x)T) - 1 + \{\text{c.t.}\}]. \quad (26)$$

The next-to-leading (NLO) correction can be written as [29, 30]¹

$$\mathcal{L}_{\text{ferm}}^{d1}(x) = C_{d1} \frac{(\partial_i B(x))^2}{B^\alpha(x)} \int_0^\infty \frac{d\omega}{\omega^\rho} e^{-\frac{m^2}{B(x)}\omega} \frac{d^3}{d\omega^3} [\omega \coth(\omega)]. \quad (27)$$

The sum of both Lagrangians provides us with the NLO derivative expansion of the fermion-induced effective Lagrangian. The prefactors $C_{d0,1}$ and exponents α , ν and ρ depend on the number D of spacetime dimensions and are summarized in Table 1. Note that the counter term $\{\text{c.t.}\} = -\frac{1}{3}(B(x)T)^2$ must be added to the integrand in Eq. (26) for $D=3+1$, as discussed in Sect. 2.2 (cf. Eq. (9)); for $D = 2 + 1$, there is no counterterm, $\{\text{c.t.}\} = 0$.

The expression (27) is valid for any value of the ratio m^2/B , i.e., *either* m^2 *or* B has to be large compared with the inverse length scale squared set by the variation of the background field. Near the vortex core, this length scale is naturally given by the core size d . For a flux $\varphi = \mathcal{O}(1)$ considered in the following, we find from Eq. (23) that $B(x)d^2 = \mathcal{O}(1)$ near the core. Simultaneously assuming small masses, $md \lesssim 1$, neither

¹A representation of the integral in terms of the Hurwitz Zeta function as well as asymptotic expansions have been found; see, for example, [30].

	$D=2+1$	$D=3+1$
C_{d0}	$\frac{1}{4\pi^{3/2}}$	$\frac{1}{8\pi^2}$
C_{d1}	$\frac{1}{4(4\pi)^{3/2}}$	$\frac{1}{(8\pi)^2}$
α	1.5	1
ν	2.5	3
ρ	0.5	1

Table 1: Prefactors and exponents of the derivative expansion.

of the possible derivative expansion parameters is small. The NLO Lagrangian reaches its validity limit, and one cannot expect reliable results from the derivative expansion. Below, it will turn out that the quality of the NLO approximation strongly depends on the number of spacetime dimensions. By contrast, for large masses $md \gg 1$ or for large radial distances from the vortex core $\rho \gg d$, we expect the NLO Lagrangian to give a reasonable answer, since one of the possible expansion parameters is small. Below, we will use the regime of large masses (or large ρ) to gain insight into the range of parameters to which worldline numerics is reliably applicable (see [21] and [25] for a first comparison of worldline numerics to the constant-field case).

4.2 Worldline numerics: $D = 2 + 1$

Closely following the procedure outlined in [21], we generate a loop ensemble with n_e loops, where each loop is represented by a set of N spacetime points with coordinates $x_1 \dots x_N$. The loop ensembles are generated with appropriate measure (see discussion in subsection 2.1). We have used 10.000 and 20.000 dummy sweeps and found that for a proper thermalization, 10.000 dummy sweeps are sufficient for the accuracy achieved in the results shown below. Furthermore, we have used $N \in 100, 150, 200$ points specifying each loop. Whereas $N = 100$ seems sufficient for our purposes in the (2+1)-dimensional case, we take $N = 200$ to generate high-precision data for the case $D = 3 + 1$. Generically, we average over $n_e = 1000$ loop ensembles in the (2+1)-dimensional case, and exceptionally use $n_e = 16000$ for certain applications in $D = 3 + 1$. Any dimensionful quantity quoted in the following is calculated in the simulation in units of vortex thickness d .

In order to avoid a violation of gauge invariance in the numerical computation, we have to deal with a subtlety concerning the discretization of the integrals along the worldlines: a particular loop in our ensemble is considered to be a polygon with straight lines C_i connecting the points x_i and x_{i+1} . In order to evaluate the holonomy in Eq. (4), we consider the “infinitesimal” part

$$\exp \left\{ i \int_{C_i} A_\mu(x) \dot{x}_\mu d\tau \right\} \quad (28)$$

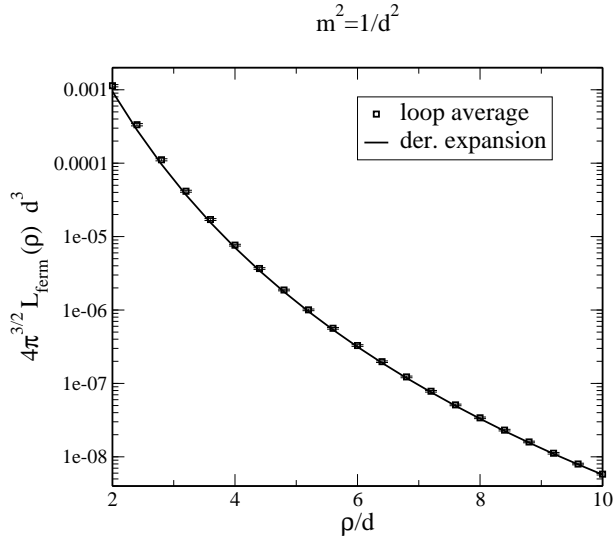


Figure 1: Effective Lagrangian as a function of the radial distance ρ to the vortex core for the case $m=1$, $\varphi=1$, $D=2+1$. The NLO derivative expansion (solid line) is compared with the numerical computation (squares with error bars).

for each \mathcal{C}_i separately and evaluate the integral analytically using the vortex profile under consideration. This procedure guarantees that our numerical result is invariant under gauge transformations of the background gauge field $A_\mu(x)$ for any number N of points defining the polygons. Moreover, the flux enclosed by the polygon is exactly taken into account as desired (and not only within discretization errors). Of course, this procedure can be generalized to arbitrary vortex profiles for which the “infinitesimal” integrations along the \mathcal{C}_i ’s can be performed numerically; thereby, the properties mentioned above can be preserved to any numerically desired precision. However, we should stress that the use of a smooth gauge (e.g., covariant gauges) for the background field is recommended in this case; this facilitates a fast convergence of the numerical integration.

In order to test our numerical approach, we calculate the effective Lagrangian $\mathcal{L}_{\text{ferm}}(\rho)$ for large values of ρ , $\rho \gg d$, where the derivative expansion is expected to give reliable results. The result of the numerical worldline approach is compared with the derivative expansion in Fig. 1 for $D = 2 + 1$. The agreement between the two curves is satisfactory; in particular, the numerical approach is able to compute $\mathcal{L}_{\text{ferm}}$ over a range of many orders of magnitude. In the region close to the core of the vortex, i.e., $\rho \approx d$, the gradients of the background field are as large as the field itself, so that the reliability of the derivative expansion now depends on the value of the mass. Our numerical findings for this regime are shown in Fig. 2 for $m^2 = 1$ (left panel) and $m^2 = 5$ (right panel). For larger masses, we observe a good qualitative and a reasonable quantitative agreement. But even for the small mass value $m^2 = 1$, there is at least qualitative agreement between the numerical result and the derivative expansion, indicating that the applicability of the derivative expansion can be pushed to its formal validity limit in $D = 2 + 1$. This observation is also supported by

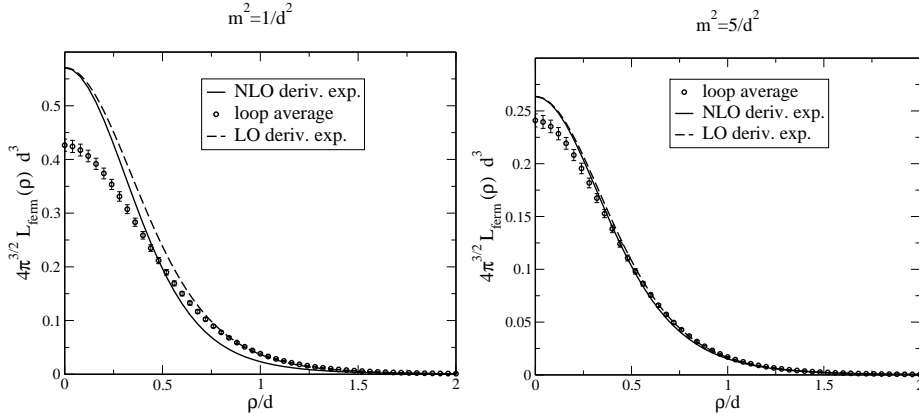


Figure 2: Effective Lagrangian in the small ρ region for the cases $m=1$ (left panel) and $m^2=5$ (right panel), $\varphi=1$, $D=2+1$.

the fact that the NLO term (27) is only a small correction to the zeroth-order result (26). Moreover, we expect that the (up to now unknown) NNLO correction, which is sensitive to the curvature of the field strength, improves the result near the vortex core. In this sense, it is reassuring to observe that the numerical result agrees with the NLO derivative expansion precisely at the turning point of the curve at $\rho \simeq 0.5$, because the NNLO correction must vanish here. We should finally stress that for even smaller masses $m < 1$, the discrepancy between our numerical result and the derivative expansion increases, so that the derivative expansion should be abandoned here.

Let us now examine the fermion-induced quantum energy E of the vortex soliton as defined in Eq. (24),

$$E = \Gamma_{\text{ferm}}^{(3)}/L_t = 2\pi \int_0^\infty d\rho \rho \mathcal{L}_{\text{ferm}}(\rho), \quad (29)$$

which we obtain by numerically integrating the effective Lagrangian. Our result for this energy is shown in Fig. 3 as function of the fermion mass m in units of the vortex thickness d . Since fermion fluctuations are suppressed with increasing mass, the quantum energy decreases with increasing m , and vanishes in the large mass limit. For phenomenological purposes, it is important to notice that the quantum energy is positive. This implies that potential effective models for vortex dynamics have to account for the fact that vortex nucleation is suppressed by the fermion-induced effective action in $D = 2 + 1$ dimensions.

Furthermore, let us consider the variation of the quantum energy with respect to the flux ϕ , which is carried by the vortex. Our numerical result is shown in Fig. 3 (right panel). We find that the energy is monotonically increasing with the flux ϕ . For $\phi \equiv \varphi\pi=2\pi$, the vortex configuration approaches asymptotically ($\rho \rightarrow \infty$) a pure gauge. As in the instanton case, the energy is nonvanishing due to the finite extension of the vortex core. It is interesting to compare our result for $E(\varphi)$ with a general result for fermionic determinants described by M. Fry in [31]; therein a lower bound has been derived for unidirectional magnetic fields in $D = 2 + 1$, which translates into an upper bound E_b for the quantum energy of our vortex

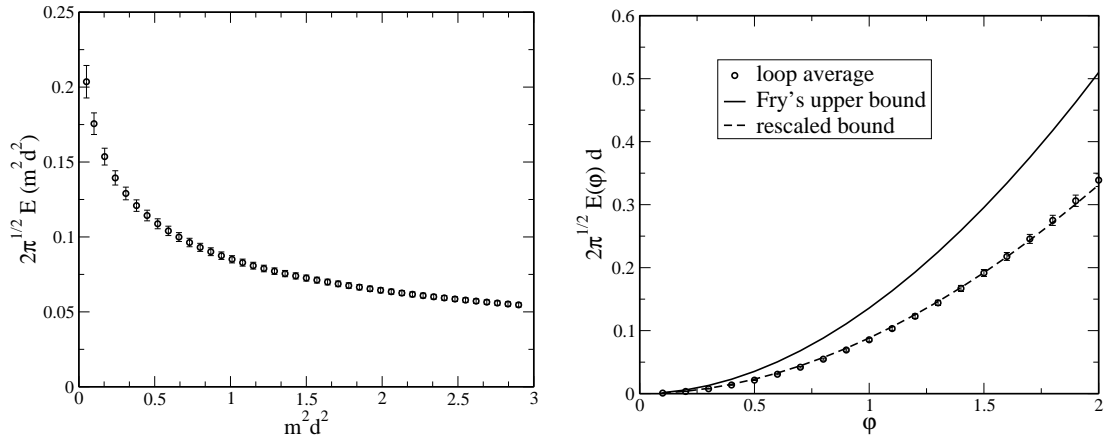


Figure 3: Quantum energy as a function of the mass m^2 for $\varphi=1$ (left panel) and as a function of the flux φ carried by the vortex for $m = 1$ (right panel) in comparison with Fry's upper bound given in Eq. (30).

configuration given by

$$\begin{aligned}
 E(\varphi) &\leq E_b(\varphi), \\
 E_b(\varphi) &= \left(\frac{1}{d}\right) \frac{1}{6} \left[2 - 3\varphi - 2\sqrt{1+\varphi} + \varphi\sqrt{1+\varphi} + 3\sqrt{\varphi} \operatorname{Arsinh}(\sqrt{\varphi}) \right]
 \end{aligned}
 \tag{30}$$

for the case $md = 1$ and Dirac 4-component spinors. For other values of md , this formula receives a total factor of $(md)^3$ and the flux has to be replaced by $\varphi \rightarrow \varphi/(md)^2$. As shown in Fig. 3, our numerical result lies well within this bound. More remarkable is the fact that the functional dependence of our result agrees with the bound within the error bars, if the bound is scaled by a factor of roughly 0.65.

As a further check, we have compared all our above-mentioned results with those of [19], where the single-vortex case with profile functions different from ours was considered within the phase-shift approach. We find good agreement within the error bars except for a global factor of 2 by which the result of [19] for $E(\varphi)$ is larger.

Let us finally point to a problematic feature of our present approach. Note that our statistical error bars increase in the regime of small fermion masses in Fig. 3 (left panel), which has the following origin: the Pauli term in Eq. (4),

$$\operatorname{tr} P_T \exp \left(\frac{1}{2} \int_0^T d\tau \sigma_{\mu\nu} F^{\mu\nu} \right),$$

can favor large loops ($T \gg d^2$) for the present unidirectional magnetic field. On the other hand, the holonomy factor,

$$\exp \left\{ i \int_0^T A_\mu(x) \dot{x}_\mu d\tau \right\},$$

changes its sign rapidly in this case when the loop under consideration is slightly deformed. This implies that a finite result in the small-mass regime arises after subtle cancellations,

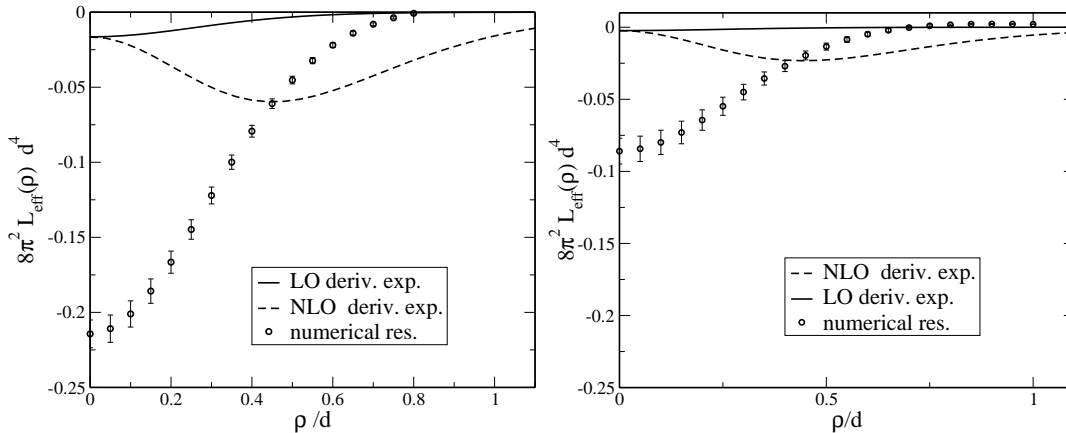


Figure 4: Effective Lagrangian for $m^2 = 1$ (left panel) and $m^2 = 3$ (right panel), $\varphi=1$, $D = 3 + 1$.

and is therefore hardly accessible to the present numerical formulation. For finite values of the mass, potentially large Pauli term contributions are suppressed by the factor $\exp(-m^2 T)$, which solves the numerical problem for large loops (large T).² However, this cancellation problem can become serious for the approach to the chiral limit; here, a solution to the problem has to be implemented in the algorithm on the analytical level rather than by brute-force numerical means.

4.3 Worldline numerics: $D = 3 + 1$

Similarly to the previous studies of the $D = 2 + 1$ case, we investigate the effective Lagrangian $\mathcal{L}_{\text{ferm}}$ as a function of ρ and compare the result with the one obtained from the derivative expansion (26,27) (see Fig. 4). Contrary to $D = 2 + 1$, we observe that unless $\rho \gg d$, the leading order (LO) of the derivative expansion falls far too short of reproducing the numerical result for $m^2 = \mathcal{O}(1)$. For instance, for $m^2 = 1$, we find an order-of-magnitude difference at $\rho = 0$ (Fig. 4 (left panel)). Moreover, the NLO contribution of the derivative expansion also exceeds the leading order result by almost an order of magnitude for $\rho \approx d$. This signals the break-down of the derivative expansion for the case of the field, its gradient and the mass being all of the same order. Contrary to the case of $D = 2 + 1$, the applicability of the NLO derivative expansion cannot be pushed to its formal validity limits $md \approx 1$. Even for larger values of the mass, $m^2 = 3$ (right panel), there is only a minor improvement of the quality of the NLO derivative expansion. Of course, the NNLO contribution could, in principle, improve the results of the derivative expansion, but this would only emphasize the fact that there is no clear hierarchy from term to term in the

²In the constant-field case, this cancellation problem already occurs for $m^2 \lesssim B$ as observed in [22]. In the present vortex case, we can afford much smaller masses. In general, the smaller the coherence length of the field, the less serious the cancellation problem. The usually considered homogeneous and unidirectional field configurations are therefore rather pathological in this respect.

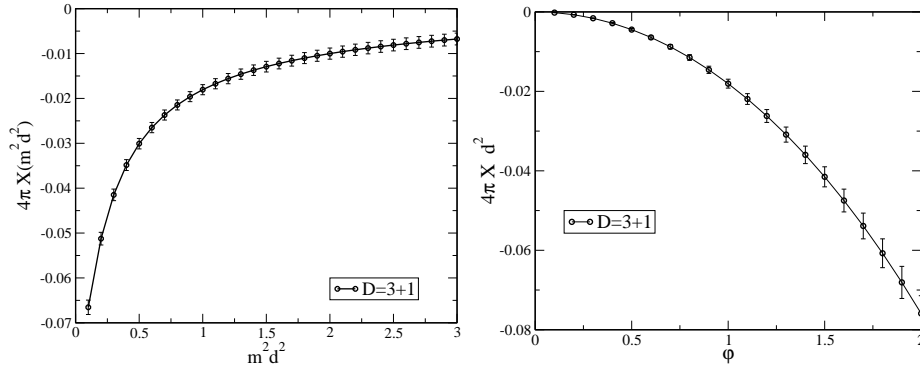


Figure 5: Effective action as a function of the dimensionless quantity m^2d^2 , $\varphi=1$, $D=3+1$ (left panel), and as function of the flux, $m^2d^2 = 1$ (right panel).

derivative expansion.

We believe that the striking difference to the $D = 2 + 1$ dimensional case is indeed remarkable and points to a deeper reason in terms of a renormalization effect. To illustrate this, we note that the quantity $\langle W_{\text{spin}} - 1 \rangle$ occurring in the proper-time integrand is positive for the vortex background, whereas the counterterm $-\frac{1}{3}B^2(x)T^2$ is negative. Since the effective Lagrangian is largely negative as seen in Fig. 4, it is mainly driven by the counterterm. Now the leading-order derivative expansion obviously overestimates the value of $\langle W_{\text{spin}} - 1 \rangle$ near the vortex core, since it is a local expansion. The true value as seen in the numerical computation is much smaller because it is a nonlocal average over the extended *loop cloud* that also “feels” the much weaker field at a radial distance from the core. The final value of the total effective Lagrangian at a point x therefore results from a nontrivial interplay between nonlocal (and nonlinear) vacuum polarization ($\sim \langle W_{\text{spin}} - 1 \rangle$) and a local definition of the coupling giving rise to a local counterterm. In regions where the background field varies rapidly, such as the near vortex core in our case, this interplay can lead to an order-of-magnitude enhancement of the effective Lagrangian as compared with the constant-field approximation (leading-order derivative expansion). In our opinion, this phenomenon clearly deserves further investigation.

Returning to our numerical study of the one-vortex background, we calculate the string tension χ as defined in Eq. (25) as a function of the fermion mass m and plot it in Fig. 5 for $\varphi = 1$. The negative values of χ show that the fermion-induced effective action Γ_{ferm} favors the nucleation of vortices. Since the modulus of this effective action increases if the vortex thickness d is decreased, the fermionic part of the vortex action supports the existence of thin vortices. These results are in contrast to those of the case $D = 2 + 1$, where the effective action turned out to be positive (see Fig. 3). This sign difference is again related to renormalization effects mediated by the counterterm.

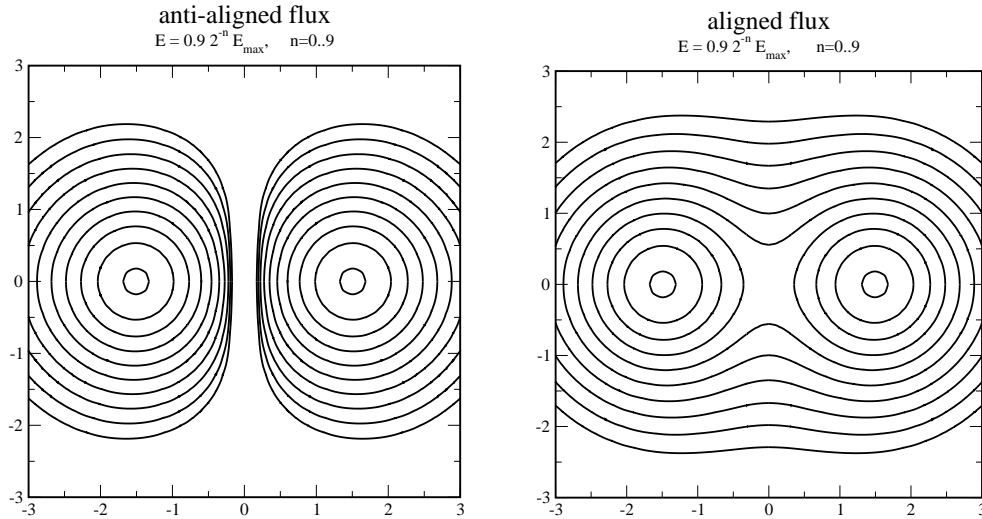


Figure 6: Effective Lagrangian $L_{\text{ferm}}^{(3)}(x, y)$ as function of the xy -plane for the two vortex configuration: parallel (right panel) and anti-parallel (left panel) orientation of the flux, $m^2 d^2 = 0.5$, $\varphi=1$, $D=2+1$.

5 Binary-vortex interactions

Since we are investigating the case of Abelian gauge configurations, the binary-vortex configuration is given by the superposition of two single vortex gauge fields $A_\mu(x)$ (22),

$$A_\mu^{(2)}(x) = A_\mu\left(x - \frac{l}{2}\right) \pm A_\mu\left(x + \frac{l}{2}\right), \quad (31)$$

where l denotes the vortex distance. Below, we will study the case of the so-called center vortices the flux of which is given by $\varphi = 1$. The relative sign between the gauge fields on the right-hand side of Eq. (31) corresponds to the relative orientation of the fluxes: the plus sign corresponds to an equal orientation of the flux in each vortex, while the minus sign signals an opposite orientation.

Figure 6 shows the lines of equal effective Lagrangian $L_{\text{eff}}^{(3)}(x, y)$ in the xy -plane which is perpendicular to the vortex fluxes. The vortices are located at the x axis at a distance $l = 3d$. It is straightforward (but computer time consuming) to integrate the effective action over the xy -plane in order to derive the quantum energy E (24) of the binary-vortex configuration. The result is shown in Fig. 7 for the case $D = 2 + 1$. For large distances $l \gg d$, the quantum energy approaches twice the value of a single vortex. For $l = 0$, the vortices fall on top of each other. If the fluxes of the vortices are oppositely oriented, the vortices annihilate each other, and the quantum energy of the configuration vanishes. If the vortex fluxes are equally oriented, the configuration is equivalent to the single vortex configuration with flux $\varphi = 2$. Since the quantum energy is roughly proportional to φ^2 (see Fig. 3), the vortex configuration with flux $\varphi = 2$ possesses a higher energy than twice the energy of a single vortex, carrying flux $\varphi = 1$. Hence, vortices with an equal flux

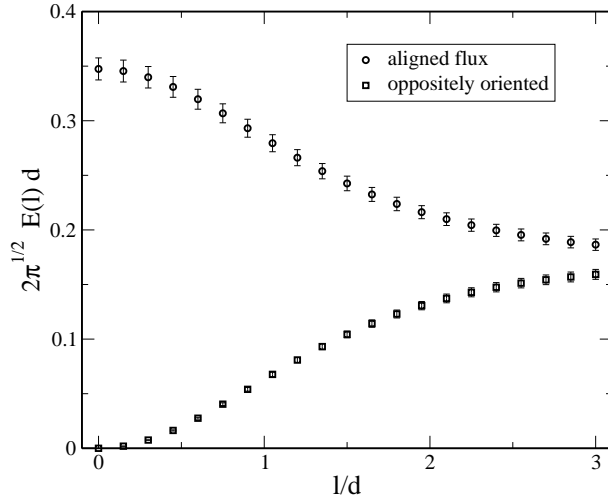


Figure 7: The interaction of two parallel vortex lines in $D = 2 + 1$, $\varphi = 1$, $m^2 d^2 = 1$.

orientation repel each other in $D = 2 + 1$, while vortices with oppositely oriented flux attract each other. The same line of argument applies to the case $D = 3 + 1$. Since the fermionic contribution to the effective action is negative in this case, the fermion-induced force is attractive (repulsive) for equally (oppositely) oriented vortices, contrary to the $D = 2 + 1$ case.

6 Fermion condensation in a vortex gas

The fermion condensate can be related to the effective action Γ_{eff} (17) by differentiation with respect to the fermion mass m ,

$$\int d^D x_0 \langle \bar{\psi} \psi \rangle = -\frac{\partial \Gamma_{\text{eff}}}{\partial m}. \quad (32)$$

Let us concentrate on $D = 3 + 1$ dimensions in the following. Here the condensate reads in worldline representation:

$$m \int d^4 x_0 \langle \bar{\psi} \psi \rangle = \frac{m^2}{4\pi^2} \int d^4 x_0 \int_0^\infty \frac{dT}{T^2} e^{-m^2 T} \left\langle W_{\text{spin}}[A] - 1 \right\rangle_x, \quad (33)$$

where we have first performed the mass differentiation at an arbitrary renormalization point and then implicitly chosen on-shell renormalization.

In the present section, we intend to estimate the quark condensate which is generated by a dilute gas of vortices of flux $\varphi = 1$ in $D = 3 + 1$. For this purpose, we first calculate the contribution of the single-vortex configuration with the help of Eq. (33). Due to translation invariance of our single-vortex background, the string tension χ (25) is provided in units

of the vortex core size only. This allows us to define the dimensionless function c_0 by

$$m \int d^4x_0 \langle \bar{\psi}\psi \rangle_{(1)} = L_t L_z \frac{m^2}{4\pi^2} c_0(m^2 d^2), \quad (34)$$

where c_0 can directly be obtained from worldline numerics,

$$c_0(m^2 d^2) = 2\pi \int_0^\infty d\left(\frac{\rho}{d}\right) \frac{\rho}{d} \int_0^\infty \frac{d\hat{T}}{\hat{T}^2} e^{-(md)^2 \hat{T}} \left\langle W_{\text{spin}}[A d] - 1 \right\rangle_x. \quad (35)$$

Here all dimensionful quantities are scaled in units of the core size d , e.g., $\hat{T} = T/d^2$, and $\rho = \sqrt{x^2 + y^2}$ measures the radial distance from the vortex core. In the following, we are interested in a dilute gas of vortices which are static and aligned in the z direction, but intersect the xy plane at random locations with random fluxes $\varphi = \pm 1$. In this plane the vortex gas can be characterized by a planar vortex area density ρ_V , which is the average number of vortices per xy unit area. The total number of vortices within the 4-dimensional spacetime is given by $N_V = \rho_V L_x L_y$. We expect the dilute-gas approximation to give reasonable results, if the average distance between two neighboring vortices is at least $\gtrsim 2d$, where the fermion-induced vortex interactions become small (see, e.g., Fig. 7 for the $D = 2 + 1$ dimensional analogue). In other words, there should be less than one vortex per core-size area, $\rho_V (\pi d^2) \lesssim 1$. In this dilute-gas approximation, the fermion condensate averaged over spacetime volume V is therefore given by

$$\langle \bar{\psi}\psi \rangle \approx \frac{1}{V} N_V \int d^4x_0 \langle \bar{\psi}\psi \rangle_{(1)} = \frac{1}{4\pi^2} m \rho_V c_0(m^2 d^2). \quad (36)$$

In the limit of large fermion masses ($m \gg 1/d$), Eq. (35) can be studied analytically with the aid of the heat-kernel expansion (8), and we find a contribution to the condensate which is subleading in $1/m$:

$$\langle \bar{\psi}\psi \rangle \approx \frac{1}{24\pi^2} \frac{1}{m} \frac{1}{V} \int d^4x_0 F^2(x_0) + \mathcal{O}\left(1/m^2\right). \quad (37)$$

Here, we recover the familiar result [32] that in the large- m limit the fermion condensate is proportional to the field strength squared of the background field (i.e., “gluon condensate” in a QCD-like language).

We investigate numerically the interesting regime of small masses m , where the heat-kernel expansion breaks down. The representation (35) is highly convenient for this purpose. However, as already pointed out, the loop average $\langle \dots \rangle$ in Eq. (34) is plagued from a severe cancellation problem which in the present case of the loop parameters employed here limits the region of validity to $T/d^2 \lesssim 100$. In order to ensure this limit, we confine ourselves to the mass range $m^2 T_{\text{max}} \geq 10$, i.e., $m^2 > 0.1/d^2$. The investigation of the small mass regime ($m^2 < 0.1/d^2$) clearly needs further study. Work in this direction is in progress [33].

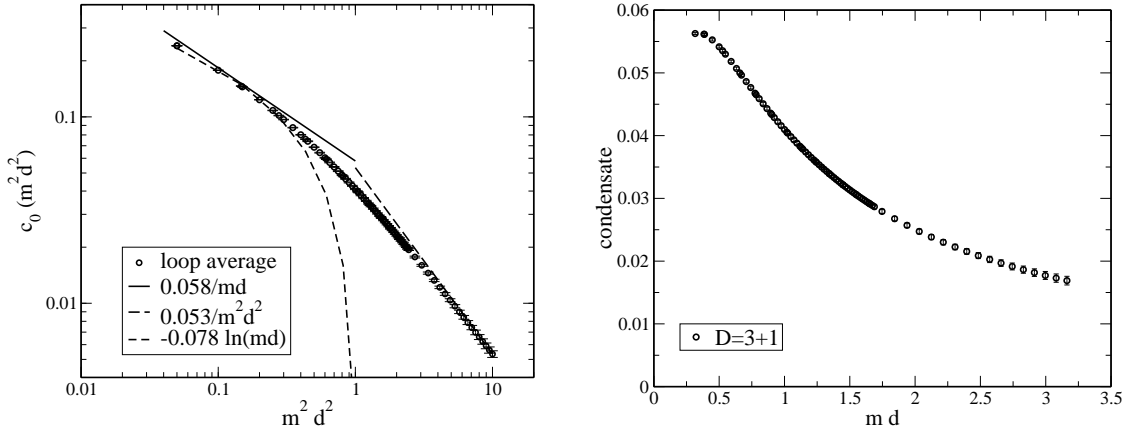


Figure 8: c_0 (34) (left panel) and the fermion condensate (right panel) as function of the fermion mass m , $\varphi=1$, $D=3+1$.

Our numerical result for c_0 is presented in Fig. 8. For small masses, i.e., $0.1 < m^2 d^2 < 0.5$, we find that $c_0(m^2 d^2) \sim 1/(md)$, which indicates that the condensate approaches a plateau in this regime according to Eq. (36),

$$\langle \bar{\psi}\psi \rangle \Big|_{m^2 d^2 = \mathcal{O}(0.1)} \approx \frac{1}{4\pi^2} m \rho c_0(m^2 d^2) \Big|_{m^2 d^2 = \mathcal{O}(0.1)} \approx 0.058 \frac{1}{4\pi^2} \rho / d, \quad (38)$$

as depicted in Fig. 8 (right panel). However, we do not believe that this result extends to the chiral limit $m \rightarrow 0$. Guided by the case of a constant background field in $D = 3 + 1$ [35], we expect that the chiral condensate vanishes according to $\langle \bar{\psi}\psi \rangle \rightarrow m \ln m$ for $m \rightarrow 0$. As seen from Fig. 8, our numerical result for c_0 does not discriminate between the $\ln m$ and the desired $1/m$ behavior in the small-mass regime.

Let us stress the two main findings of this subsection: first, the vortex-gas-induced condensate is characterized by a comparably low value of c_0 for all mass values depicted above and an onset of the plateau value for comparably large masses $m^2 d^2 \sim 0.1$; we point out that it is not possible to fit the form of the condensate depicted above within a derivative expansion even qualitatively by arbitrarily varying B . Second, in the context of a center vortex model for low-energy QCD, the current quark masses are in fact finite, though small. The present result indicates that contributions to the chiral condensate have to be expected from an interaction of the massive quarks with the gauge vacuum (modeled by a random vortex background). As a first estimate, we may insert parameter values known from lattice calculations. In the case of an $SU(2)$ gauge theory, the density of the center vortices is roughly given by $\rho_V = 3.6/\text{fm}^2$. The planar vortex correlation function was also studied in $SU(2)$ lattice gauge theory [34]. One finds an exponential decrease of the correlation function. This allows for a definition of a vortex thickness of $d \approx 0.3 \dots 0.4 \text{ fm}$. Since $\rho_V \pi d^2 = \mathcal{O}(0.1)$ in this case, the dilute-gas approximation should be applicable. From Eq. (38), we find for the vortex-induced condensate $\langle \bar{q}q \rangle \approx [50 \text{ MeV}]^3$, for masses $m^2 d^2 = 0.1$, i.e., $m \simeq 100 \text{ MeV}$. As discussed above, the present algorithm cannot treat the case of light mass values, $m \simeq 5 \dots 10 \text{ MeV}$.

The vortices considered here obviously possess a trivial topology, i.e., they do not contribute to the topological charge. The origin of a chiral condensate here is entirely relegated to the field strength carried by the vortex cores. In a fully non-Abelian QCD-like context, topologically non-trivial vortex configurations (due to the presence of low-lying fermionic modes of the Dirac operator) as well as multi-gluon exchange interactions can be expected to provide for a drastic enhancement of the condensate.

7 Conclusions

The fermion-induced quantum action of Abelian vortex configurations has been studied in the case of $D = 2 + 1$ and $D = 3 + 1$ dimensions using worldline numerics [21, 22, 25]. The quantum action of a single-vortex configuration is characterized by the fermion mass m , the vortex thickness d and the flux φ carried by the vortex. Our numerical approach has been successfully tested in the parameter regime where the derivative expansion is expected to provide reliable results: in the large-mass regime $md \gg 1$ or for strong-field suppression of the inhomogeneities $\partial^2/B \ll 1$.

Compared with our numerical results in $D = 2 + 1$, the derivative expansion provides for a reasonable approximation to the quantum energy of a single vortex configuration even for smaller masses, $md \lesssim 1$. The next-to-leading order only adds a small correction to the leading-order result. By contrast, in $D = 3 + 1$, the derivative expansion is insufficient even for comparably large masses, $md = \mathcal{O}(5)$. Only for very large masses, $md \gg 1$, can the derivative expansion be trusted. We have argued that this disparity between $D = 2 + 1$ and $D = 3 + 1$ arises from renormalization effects in the latter case, which can occur near regions where the background varies rapidly. In particular, these renormalization effects can lead to an effective enhancement of the quantum action. Further investigations are planned to settle this issue.

From a physical point of view, we find that the quantum action is positive in $D = 2 + 1$, implying that the presence of vortices is suppressed, and large vortex core sizes d are preferred. In $D = 3 + 1$, the properly renormalized quantum action turns out to be negative: the nucleation of thin ($d \rightarrow 0$) vortices in $D = 3 + 1$ is supported by the fermion induced quantum action.

Subsequently, the binary-vortex interaction was investigated. We found that the fermion-induced interaction favors vortices with an opposite orientation of the fluxes in $D = 2 + 1$, while in $D = 3 + 1$, a unique orientation of the fluxes is preferred.

It should be stressed that these statements refer to and are derived from the fermion-induced action. In a pure QED context, the classical action has to be taken into account. The latter will dominate the fermion-induced action by far at weak coupling, reflecting the usual hierarchy between classical and quantum-induced nonlinear electrodynamics. Formally, the classical and quantum action can become comparable in magnitude for exponentially strong fields in the vortex core (exponentially small d for fixed flux); however, this is nothing but a manifestation of the Landau pole of QED and thus should be rated as unphysical.

Finally, the fermion condensate which is generated by a dilute gas of vortices was studied as function of the fermion mass $md > 0.1$ in $D = 3 + 1$. We found that the condensate decreases like $1/m$ for large values of the mass and that it reaches a plateau for $md \lesssim 0.5$. Similarly to the case of a constant magnetic field, we expect that the condensate vanishes like $m \ln m$ in the chiral limit $m \rightarrow 0$. However, our results point to an interesting phenomenon: although chiral symmetry breaking might be tied to topological properties of the background fields not covered by the present considerations, the field strength carried by the vortex cores enhances the chiral condensate in the intermediate fermion mass regime. In a center vortex model of low-energy QCD, this effect may lead to a nonnegligible contribution to the condensate. We regret that our worldline numerical algorithm in its present form cannot address the small-mass regime $md < 0.1$ due to severe cancellations. The study of the chiral limit in general and chiral symmetry breaking by vortex background fields in particular requires improved algorithms and is left to future work [33].

Acknowledgments:

The authors are grateful to W. Dittrich, H. Reinhardt and H. Weigel for helpful discussions and detailed comments on the manuscript. H.G. acknowledges the support of the Deutsche Forschungsgemeinschaft under contract Gi 328/1-1. L.M. was supported by the Deutsche Forschungsgemeinschaft under contract GRK683.

References

- [1] D. B. Kaplan, Phys. Lett. B **288**, 342 (1992) [arXiv:hep-lat/9206013].
- [2] Y. Kikukawa, Nucl. Phys. B **584**, 511 (2000) [arXiv:hep-lat/9912056].
- [3] P. Chen *et al.*, Phys. Rev. D **59**, 054508 (1999) [arXiv:hep-lat/9807029].
- [4] V. A. Rubakov, Phys. Usp. **44**, 871 (2001) [Usp. Fiz. Nauk **171**, 913 (2001)] [arXiv:hep-ph/0104152].
- [5] G. W. Crabtree, D. R. Nelson, Physics Today **50** (1997) 38.
- [6] K. Langfeld, H. Reinhardt and O. Tennert, Phys. Lett. B **419**, 317 (1998) [arXiv:hep-lat/9710068].
- [7] L. Del Debbio, M. Faber, J. Greensite and S. Olejnik, Nucl. Phys. Proc. Suppl. **53**, 141 (1997) [arXiv:hep-lat/9607053].
- [8] L. Del Debbio, M. Faber, J. Giedt, J. Greensite and S. Olejnik, Phys. Rev. D **58**, 094501 (1998) [arXiv:hep-lat/9801027].
- [9] K. Langfeld, O. Tennert, M. Engelhardt and H. Reinhardt, Phys. Lett. B **452**, 301 (1999) [arXiv:hep-lat/9805002].
- [10] M. Engelhardt, K. Langfeld, H. Reinhardt and O. Tennert, Phys. Rev. D **61**, 054504 (2000) [arXiv:hep-lat/9904004].
- [11] T. G. Kovacs and E. T. Tomboulis, Nucl. Phys. Proc. Suppl. **106**, 670 (2002) [arXiv:hep-lat/0110123], and arXiv:hep-lat/0108017.

- [12] M. Engelhardt and H. Reinhardt, Nucl. Phys. B **585**, 591 (2000) [arXiv:hep-lat/9912003].
- [13] M. Engelhardt, Nucl. Phys. B **585**, 614 (2000) [arXiv:hep-lat/0004013].
- [14] N. Graham, R. L. Jaffe and H. Weigel, Int. J. Mod. Phys. A **17**, 846 (2002) [arXiv:hep-th/0201148].
- [15] N. Graham, R. L. Jaffe, M. Quandt and H. Weigel, Phys. Rev. Lett. **87**, 131601 (2001) [arXiv:hep-th/0103010].
- [16] F. Gygi, M. Schlüter, Phys. Rev. **B43** (1991) 7609.
- [17] N. Schopohl, K. Maki, Phys. Rev. **B52** (1995) 490;
N. Schopohl, cond-mat/9804064.
- [18] P. Gornicki, Annals Phys. **202**, 271 (1990);
Y. A. Sitenko and A. Y. Babansky, Mod. Phys. Lett. A **13**, 379 (1998) [arXiv:hep-th/9710183].
- [19] P. Pasipoularides, Phys. Rev. D **64**, 105011 (2001) [arXiv:hep-th/0012031].
- [20] M. Bordag and K. Kirsten, Phys. Rev. D **60**, 105019 (1999) [arXiv:hep-th/9812060].
- [21] H. Gies and K. Langfeld, Nucl. Phys. B **613**, 353 (2001) [arXiv:hep-ph/0102185].
- [22] H. Gies and K. Langfeld, Int. J. Mod. Phys. A **17**, 966 (2002) [arXiv:hep-ph/0112198].
- [23] Z. Bern and D. A. Kosower, Phys. Rev. Lett. **66**, 1669 (1991);
Nucl. Phys. B **379**, 451 (1992); M. J. Strassler, Nucl. Phys. B **385**, 145 (1992) [arXiv:hep-ph/9205205]; A. M. Polyakov, “Gauge Fields And Strings,” *Chur, Switzerland: Harwood (1987) (Contemporary Concepts In Physics, 3)*.
- [24] C. Schubert, Phys. Rept. **355**, 73 (2001) [arXiv:hep-th/0101036].
- [25] M. G. Schmidt and I. O. Stamatescu, arXiv:hep-lat/0201002.
- [26] D. Diakonov, Mod. Phys. Lett. A **14**, 1725 (1999) [arXiv:hep-th/9905084].
- [27] W. Heisenberg and H. Euler, Z. Phys. **98**, 714 (1936).
- [28] J. Schwinger, Phys. Rev. **82**, 664 (1951)
- [29] D. Cangemi, E. D’Hoker and G. V. Dunne, Phys. Rev. D **51**, 2513 (1995) [arXiv:hep-th/9409113].
- [30] V. P. Gusynin and I. A. Shovkovy, J. Math. Phys. **40**, 5406 (1999) [arXiv:hep-th/9804143].
- [31] M. P. Fry, Phys. Rev. D **54**, 6444 (1996) [arXiv:hep-th/9606037].
- [32] M. A. Shifman, A. I. Vainshtein, V. I. Zakharov, Nucl. Phys. **B147** (1979) 385;
- [33] L. Moyaerts, H. Reinhardt, H. Gies, K. Langfeld, work in progress.
- [34] M. Engelhardt, K. Langfeld, H. Reinhardt and O. Tennert, Phys. Lett. B **431**, 141 (1998) [arXiv:hep-lat/9801030].
- [35] W. Dittrich and M. Sieber, J. Phys. A **21**, L711 (1988);
W. Dittrich and H. Gies, Springer Tracts Mod. Phys. **166**, 1 (2000).